

## Dislocation loops and bond-orientational order in the Abrikosov flux-line lattice

M. Cristina Marchetti\* and David R. Nelson

*Lyman Laboratory of Physics, Harvard University, Cambridge, Massachusetts 02138*

(Received 10 July 1989)

An Abrikosov flux-line lattice with an equilibrium concentration of unbound dislocation loops is considered as a way to describe the entangled flux liquid that arises in high- $T_c$  superconductors. The long-wavelength properties of this dislocation loop gas are discussed using continuum elastic theory. We show explicitly that edge dislocations drive the long-wavelength shear modulus to zero, i.e., melt the lattice, analogous to what happens in two dimensions. Dislocations do not, however, destroy the sixfold long-range orientational order of the crystal in the  $xy$  plane. The flux-line lattice with dislocations is therefore a hexatic liquid crystal of lines rather than an isotropic liquid. The expected signature of an entangled hexatic liquid from neutron diffraction is discussed. Long-range orientational order relaxes in the  $z$  direction with a correlation length due to flux-line entanglement mediated by screw dislocations.

### I. INTRODUCTION

Over the past year there has been much interest in the possibility of a new regime in the intermediate state of high- $T_c$  superconductors.<sup>1-4</sup> Theoretical estimates based on the Lindemann criterion for melting<sup>2,5</sup> predict that the high critical temperatures and weak interplanar couplings in these materials lead to flux-line lattices which are melted over a significant portion of the phase diagram. In Ref. 1 it was shown that the flux lattice must also melt near  $H_{c1}$  by mapping the statistical mechanics of thermally excited flux lines onto the physics of two-dimensional boson superfluids (for a related mapping, see Ref. 3). Melting occurs from this point of view because bosons with a purely repulsive short-range potential are always melted by zero-point motion at low density. Much of this theoretical work was inspired by flux decoration experiments<sup>6</sup> suggesting that  $\text{YBa}_2\text{Cu}_3\text{O}_7$  is melted at 77 K at low fields, and by vibrating reed experiments<sup>7</sup> indicating a melting curve in the  $(H-T)$  plane which, for  $\text{Bi}_2\text{Sr}_2\text{CaCu}_2\text{O}_8$ , lies far below the mean-field transition line  $H_{c2}(T)$ . A melting line which combines the quantitative Lindemann fits to the experimental data on Bi-Sr-Ca-Cu-O of Ref. 5 with the results of Ref. 1 sketched in Fig. 1.<sup>8,9</sup>

The theoretical picture of the statistical mechanics just sketched neglects pinning that is known to be very important in conventional superconductors. The short coherence lengths and high critical temperatures of the high- $T_c$  materials suggests, however, that pinning may be relatively unimportant over much of the phase diagram.<sup>10</sup> At very low temperatures, where pinning cannot be neglected, disorder disrupts the Abrikosov flux lattice, producing a translational correlation length whose size depends on the density and strength of the pinning centers and on the stiffness of the lattice.<sup>11</sup> Even in this case, decoration experiments<sup>12</sup> have revealed that at least some samples possess very long translational correlation lengths, despite the weakness of the elastic constants at the low fields accessible to the decoration technique.

Although some materials may exist in a highly disordered impurity-induced "vortex glass" state at low temperatures (this being especially likely in the regime of weak elastic constants near  $H_{c1}$ ), such a glass can still "melt," in the sense that vortex lines begin to move appreciably on experimental time scales at sufficiently high temperatures.<sup>13</sup> Whether this "melting" is a distinct thermodynamic phase transition<sup>4</sup> or a more gradual process,<sup>14</sup> as in conventional glasses, the resulting flux liquid should be very similar to the liquid produced by the melting of an impurity-free Abrikosov flux crystal. This liquid of lines is a new form of matter and it is of considerable interest in its own right.

It is well known that flux lattice melting can occur in conventional superconductors in two dimensions via a dislocation-mediated mechanism. Fisher<sup>15</sup> has proposed

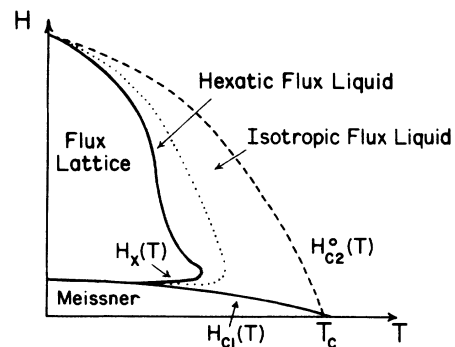


FIG. 1. Schematic phase diagram for thick single crystal samples of Bi-Sr-Ca-Cu-O for magnetic fields  $H$  directed perpendicular to the  $\text{CuO}_2$  planes. The Meissner, Abrikosov flux lattice and entangled flux liquid are shown. The melting curve  $H_x(T)$  was obtained in Ref. 8 by combining the Lindemann criterion calculations of Ref. 5 with a low-field estimate of the melting transition. The curve  $H_{c2}(T)$ , which need not be a sharp phase transition, marks the onset of the Meissner effect. The model studied here leads to an entangled hexatic phase separating the flux lattice from the entangled liquid.

a phase diagram not unlike Fig. 1 for superconducting films. Because the Kosterlitz-Thouless dislocation melting criterion estimated by Fisher is an *upper bound* on the true melting temperature, his conclusion that the melting line lies well below the mean field  $H_{c2}(T)$  curve is correct even if the melting transition is first order. The novelty of high- $T_c$  superconductors lies in the fact that flux lines can wander significantly as they traverse a bulk sample, in contrast to the rigid vortices assumed in the traditional treatment of the intermediate state of type-II superconductors.<sup>16</sup> In thick enough samples this line wandering can lead to a new entangled flux liquid regime.<sup>1</sup> This possibility arises from both the critical temperature and the anisotropy of the high- $T_c$  oxides. As a result of the weak interplanar coupling, the effective bending energy per unit length  $\bar{\epsilon}_1$  of a flux line can be much smaller than in conventional superconductors.<sup>2</sup> Flux lines are therefore quite flexible and the flux liquid will always be entangled in sufficiently thick samples. Some of the properties of this entangled liquid of line defects were discussed recently by Nelson and Seung,<sup>2</sup> on the basis of the analogy with superfluidity of boson world lines in 2+1 dimensions already mentioned.

The entanglement of the flux lines can have important consequences for the transport properties of the oxide superconductors. A heavily entangled flux liquid could exhibit viscoelastic behavior analogous to that of dense polymer melts.<sup>2</sup> This sluggish dynamics arises from the “intrinsic” randomness associated with entanglement and should be contrasted with the “extrinsic” impurity-induced glassy behavior discussed in Ref. 4. The idea of dynamical constraints associated with entanglement requires an appreciable barrier to flux-line crossing. Although this barrier will be very low near  $H_{c2}(T)$ , where the condensation energy vanishes, it was estimated to be of order  $50k_B T$  at  $T=77$  K in the high- $T_c$  materials in Ref. 2. This strongly temperature-dependent barrier<sup>17</sup> could be responsible for “irreversibility lines” like those discussed by Malozemoff *et al.*<sup>18</sup>

A glassy analogue of the entangled flux liquid was suggested for conventional superconductors some time ago by Wördenweber and Kes<sup>19</sup> and by Brandt.<sup>20,21</sup> These authors proposed that the strong pinning regime of impure superconductors would be precisely a strongly distorted “spaghetti-like” state of entangled flux lines. In this case entanglement is driven by quenched impurity disorder, rather than thermal fluctuations. Brandt pointed out the flux-line entanglement results from screw dislocations in the triangular Abrikosov flux lattice. He suggested that a heavily entangled state can be described as a lattice with a high density of screw dislocations.

Dislocations not only mediate entanglement, but when thermally activated, could provide a mechanism for melting the Abrikosov flux lattice in *three* dimensions. Dislocation melting theories in three dimensions usually postulate a free energy which depends on the dislocation line density  $\rho$  according to,<sup>22</sup>

$$F(\rho) = A\rho \ln \rho + B\rho + C\rho^2 + \dots \quad (1.1)$$

The coefficient of the term  $\rho \ln \rho$  arises from the long-

range elastic energy of the dislocations and is always positive. The linear term changes from positive to negative with increasing temperature and is due to a competition between the energy in the dislocation cores and the entropy associated with line wandering. The quadratic term has been attributed to the short-range repulsion between dislocations with parallel Burger’s vectors.<sup>22</sup> A finite density of dislocation lines appears above a first-order melting transition when  $B(T)$  becomes sufficiently negative. Although the transition to the Abrikosov flux lattice is continuous in mean-field theory,<sup>16</sup> fluctuations drive this transition first order in an expansion in  $\epsilon=6-d$ ,<sup>23</sup> consistent with the prediction of Eq. (1.1).

Here, we consider a flux-line lattice with an equilibrium concentration of unbound dislocation loops as a way of describing the entangled flux liquid. A dislocation loop in a flux-line lattice with  $\mathbf{H} \parallel \hat{z}$  is shown in Fig. 2.<sup>24</sup> These loops are highly constrained, in the sense that they must always lie in the plane defined by the  $z$  axis and their Burger’s vector.<sup>25</sup> In this paper we discuss the long-wavelength properties of this dislocation loop gas. We find that the long-wavelength shear modulus vanishes, i.e., dislocations melt the lattice. Dislocations do not, however, destroy the long-range orientational order and the dislocation gas resists deformations of the bond-angle field  $\theta(\mathbf{r})$ , where  $\theta(\mathbf{r})$  is the angle (modulo  $2\pi/6$ ) with respect to some reference axis of a line joining a vortex with its neighboring vortices in a constant  $z$  cross section.<sup>26</sup> In this sense a flux-line lattice with unbound dislocation loops is not a liquid, but is a hexatic liquid crystal of lines,<sup>27</sup> analogous to the two-dimensional hexatic proposed some time ago by Nelson and Halperin.<sup>26</sup>

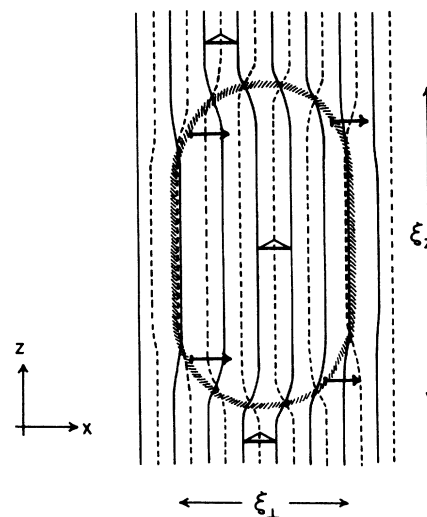


FIG. 2. A dislocation loop in the triangular flux-line lattice with  $\mathbf{H} \parallel \hat{z}$ . The Burger’s vector is in the  $x$  direction and the loop lies in the  $xz$  plane. Solid lines represent a plane of flux lines close to the viewer, dashed lines represent a plane of flux lines further away from the viewer. The aspect ratio of a typical loop in the crystalline phase is  $\xi_z/\xi_\perp \approx \sqrt{K/\mu}$ . The three triangles lie in different constant- $z$  planes, but have the same orientation, suggesting that dislocation loops have only a minor effect on bond-orientational order.

The long-range orientational order relaxes in the  $z$  direction with a finite correlation length due to flux-line entanglement caused by screw dislocations. Dislocations do not renormalize the tilt elastic constant of the lattice since they cannot relax a tilt. If flux lines are constrained not to cross and never split or merge inside the sample, there are severe constraints on the type of relaxation processes which they can mediate.

Our treatment does not address the very interesting question of the melting transition itself. We have, in particular, no explanation of the apparently continuous changes during melting observed in,<sup>7</sup> other than in terms of the crossover to two-dimensional behavior discussed in Ref. 2. We discuss the properties of a flux lattice with a finite density of dislocation lines only as a way of describing the entangled flux liquid. Our methods are adapted from a study of *cubic* bond orientational order induced by unbound dislocations in conventional bulk crystals.<sup>28</sup> The resulting cubic liquid crystal phase has never been seen, possibly because icosahedral, rather than cubic short-range order predominates in three-dimensional liquids.<sup>17</sup> The conditions for a bulk hexatic line liquid are more favorable, because of the hexagonal local coordination topology of flux lines in any plane perpendicular to the magnetic field. If the hexatic is present as an equilibrium phase in high-temperature superconductors, an additional transition line separating it from an isotropic liquid must appear, as shown in Fig. 1, just as in superconducting films.<sup>15</sup>

In Sec. II we describe some of the geometrical properties of dislocation loops in the flux-line lattice and obtain the free energy of dislocations in a continuum limit. Some of the details of the derivation are given in the Appendix. In Sec. III we discuss the static properties of a flux-line lattice with an equilibrium distribution of “unbound” dislocation loops, i.e., loops of arbitrarily large size. We show that the crystal with dislocations is a hexatic liquid crystal of lines, since the long-wavelength shear modulus vanishes and there remains long-range orientational order.

## II. DISLOCATION LOOPS IN THE FLUX-LINE LATTICE

In this section we describe the behavior of a flux-line lattice with an equilibrium density of “free” or “unbound” dislocation loops. We follow closely the method described in Ref. 28. Our starting point is a continuum description of dislocation loops embedded in the flux-line lattice. We assume that the external field is aligned with the  $z$  direction. The phonon field of the line lattice in the continuum limit is then a two-dimensional displacement vector in the  $xy$  plane,  $\mathbf{u}(\mathbf{r}) = \mathbf{u}(x, y, z)$ . The long-wavelength properties of the flux lattice are described by an elastic free energy

$$F_E = \frac{1}{2} \int d^3r \left[ 2\mu u_{ij}^2 + \lambda u_{kk}^2 + K \left[ \frac{\partial \mathbf{u}}{\partial z} \right]^2 \right], \quad (2.1)$$

where

$$u_{ij} = \frac{1}{2} \left[ \frac{\partial u_i}{\partial r_j} + \frac{\partial u_j}{\partial r_i} \right] \quad (2.2)$$

is the symmetrized two-dimensional strain matrix,  $\mu$  and  $\lambda$  are Lamé coefficients, and  $K$  is a tilt elastic constant.<sup>29</sup> The three elastic constants in (2.1) are “bare” elastic constants, unrenormalized by dislocations. It has been pointed out by Brandt<sup>21</sup> that nonlocality effects are important in the flux-line lattice and (2.1) should be replaced by a more general free energy containing wave-vector-dependent elastic constants. Here we neglect for simplicity these effects and briefly discuss their role at the conclusion of our analysis.

A dislocation line is characterized by the amount by which the integral of the displacement field along a contour enclosing the line fails to close,<sup>30,31</sup>

$$\oint du_i(\mathbf{r}) = -b_i(\mathbf{r}). \quad (2.3)$$

This defines the two-dimensional Burger’s vector  $\mathbf{b}$  of the dislocation. The direction of integration around the contour is that of a right-handed screw advancing parallel to a unit tangent vector  $\boldsymbol{\tau}$  on the line. The peculiarity of dislocation lines in the flux-line lattice is that while the Burger’s vector is two-dimensional and lies in the  $xy$  plane, the tangent  $\boldsymbol{\tau}$  to the line is a three dimensional vector.

Following standard treatments,<sup>30</sup> it can easily be shown that the Burger’s vector is constant along a line and that (2.3) can be written in an equivalent differential form,

$$\epsilon_{ijm} \frac{\partial w_{mk}(\mathbf{r})}{\partial r_j} = -\tau_i b_k \delta^{(2)}(\boldsymbol{\xi}), \quad (2.4)$$

where  $\delta^{(2)}(\boldsymbol{\xi})$  is a two-dimensional  $\delta$  function of the radius vector  $\boldsymbol{\xi}$  taken from a given point on the axis of the dislocation line in a plane perpendicular to the tangent vector  $\boldsymbol{\tau}$  and

$$w_{mk}(\mathbf{r}) = \frac{\partial u_k(\mathbf{r})}{\partial r_m}. \quad (2.5)$$

where  $m = x, y, z$  and  $k = x, y$ .

Dislocations in the triangular flux line lattice have been discussed by Nabarro and Quintanilha.<sup>25</sup> An edge dislocation is obtained by removing a half-sheet of vortex lines. Edge dislocation lines always run in the  $z$  direction and can have any Burger’s vector in the  $xy$  plane consistent with the symmetries of the triangular lattice. For instance, an edge dislocation with Burger’s vector in the  $x$  direction is obtained by removing by half-sheet of vortex lines in the  $zy'$  plane, with  $\mathbf{y}' = (\frac{1}{2}, \sqrt{3}/2, 0)$ . Edge dislocation lines with tangents in the  $xy$  plane would, however, correspond to situations where each flux line in a row merges into two lines. These are very costly in energy and we exclude them here. Screw dislocations, on the other hand, are always normal to the flux lines, i.e., they lie in the  $xy$  plane. A screw dislocation with Burger’s vector in the  $x$  direction is shown in Fig. 3. It is also apparent from Fig. 3 that screw dislocations lead to entanglement of the vortex lines, as pointed out by Brandt.<sup>20</sup>

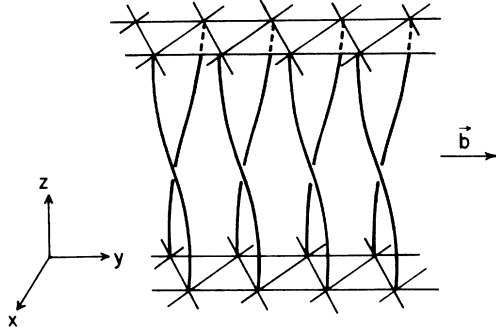


FIG. 3. A screw dislocation in the triangular flux-line lattice. The magnetic field  $\mathbf{H}$  is in the  $z$  direction and the Burger's vector is in the  $y$  direction. Screw dislocations cause flux lines to wrap around each other. A simple braiding of lines is caused by an infinite stack of screw dislocations at  $z_1 < z_2 < \dots < z_n < \dots$  with Burger's vectors  $\mathbf{b}_n = b_0(\cos \pi n/3, \sin \pi n/3)$ .

The constraint that a flux line does not split into two lines inside the sample imposes a restriction on the type of dislocation loops that are allowed in the flux-line lattice. To see this, consider a dislocation loop of Burger's vector  $\mathbf{b}$  and let  $\tau(\mathbf{r})$  be the tangent to the loop at  $\mathbf{r}$ . At all points along the loop we must have  $\tau(\mathbf{r}) \cdot (\hat{\mathbf{z}} \times \mathbf{b}) = 0$  because a nonvanishing component of  $\tau$  along  $\hat{\mathbf{z}} \times \mathbf{b}$  would correspond to an edge dislocation in the  $xy$  plane. A dislocation loop of Burger's vector  $\mathbf{b}$  lies therefore in the vertical plane spanned by  $\mathbf{H}$  and  $\mathbf{b}$ . As an example, a dislocation loop with Burger's vector in the  $x$  direction is shown in Fig. 2. The elastic energy per unit length of an edge dislocation is  $U_e \simeq (\mu b^2 / 2\pi) \ln(R/b)$ , with  $R$  a typical sample dimension, while the energy of a screw dislocation is  $U_s \simeq (\sqrt{\mu k} b^2 / 4\pi) \ln(R/b)$ . In conventional superconductors  $K \gg \mu$  and dislocation loops in equilibrium are very elongated in the  $z$  direction, i.e., have a very small screw component. In the high- $T_c$  oxides, however, the anisotropy leads to smaller values of  $K$  than in conventional materials. This makes the energies of the two types of dislocations comparable, so that loops in equilibrium can have a large screw component and line entanglement occurs.

To study properties at wavelengths long compared to the spacing between dislocation lines we use a continuum description. We average (2.4) over a small volume containing many dislocations, obtaining,

$$\epsilon_{ijm} \frac{\partial w_{mk}(\mathbf{r})}{\partial r_j} = -\alpha_{ik}(\mathbf{r}), \quad (2.6)$$

where  $i = x, y, z$  and  $k = x, y$ . The hypothesis that there is a finite concentration of unbound dislocation loops insures that many dislocation lines will enter and leave this hydrodynamic averaging volume. The tensor  $\alpha_{ik}(\mathbf{r})$  is a density of Burger's vector "charge" carried by dislocation lines piercing the averaging volume. It is defined so that its integral over a surface  $S$  spanning a contour  $C$  gives the sum of all Burger's vectors enclosed by that contour,

$$\int_S \alpha_{ik} n_i dA = \sum_{\gamma} b_k^{(\gamma)}. \quad (2.7)$$

Here  $\mathbf{n}$  is a unit vector normal to the surface and the summation over  $\gamma$  runs over those Burger's vectors encompassed by  $C$ . The density tensor  $\alpha_{ik}(\mathbf{r})$  is a measure of the number of dislocation lines with Burger's vector  $b_k$  crossing a unit area normal to the tangent  $\tau_i$ . It vanishes for  $k = z$ , since the Burger's vector always lies in the  $xy$  plane. In this continuum treatment edge dislocations are described by the components  $\alpha_{zk}(\mathbf{r})$ , for  $k = x, y$ , of the dislocation density tensor. Screw dislocations are described by the two-dimensional tensor  $\alpha_{ik}^{\perp}(\mathbf{r})$ , for  $i = x, y$  and  $k = x, y$ . The constraint that dislocation loops lie in the plane of  $\hat{\mathbf{z}}$  and  $\mathbf{b}$  translates in the requirement that the two-dimensional tensor  $\alpha_{ik}^{\perp}(\mathbf{r})$  be symmetric,

$$\epsilon_{ik} \alpha_{ik}^{\perp}(\mathbf{r}) = 0, \quad (2.8)$$

where  $\epsilon_{ik}$  is the two-dimensional antisymmetric tensor,  $\epsilon_{xy} = -\epsilon_{yx} = 1$ . When expressed as a  $3 \times 3$  matrix,  $\alpha_{ik}(\mathbf{r})$  has five independent components, because  $\alpha_{xy} = \alpha_{yx}$ ,

$$\alpha_{ik} = \begin{pmatrix} \alpha_{ik}^{\perp} & 0 \\ \alpha_{zk} & 0 \end{pmatrix} = \begin{pmatrix} \alpha_{xx} & \alpha_{xy} & 0 \\ \alpha_{xy} & \alpha_{yy} & 0 \\ \alpha_{zx} & \alpha_{zy} & 0 \end{pmatrix}. \quad (2.9)$$

There is, however, the additional constraint that dislocation loops must either close or terminate at the boundaries. This amounts to the condition,

$$\frac{\partial \alpha_{ik}(\mathbf{r})}{\partial r_i} = 0. \quad (2.10)$$

In the presence of dislocations the strain field can be written as the sum of two parts, a part,

$$\phi_{ij}(\mathbf{r}) = \frac{1}{2}(\partial_i \phi_j + \partial_j \phi_i),$$

associated with a smoothly varying two-dimensional displacement field,  $\phi(\mathbf{r})$ , and a singular part  $u_{ij}^{\text{sing}}(\mathbf{r})$  due to dislocations,

$$u_{ij}(\mathbf{r}) = \phi_{ij}(\mathbf{r}) + u_{ij}^{\text{sing}}(\mathbf{r}). \quad (2.11)$$

The free energy (2.1) then also breaks into two parts,

$$F_E = F_0 + F_D, \quad (2.12)$$

with

$$F_0 = \frac{1}{2} \int d\mathbf{r} \left[ 2\mu \phi_{ij}^2 + \lambda \phi_{kk}^2 + K \left[ \frac{\partial \phi}{\partial z} \right]^2 \right]. \quad (2.13)$$

The dislocation part is more conveniently written in terms of the Fourier transformed charge density tensor  $\alpha_{ij}(\mathbf{q})$  as

$$F_D = \frac{1}{2} \int \frac{d\mathbf{q}}{(2\pi)^3} \left[ \frac{1}{q^2} R_{ij,kl}(\mathbf{q}) + 2E_e \delta_{jl} \delta_{iz} \delta_{kz} + 2E_s \delta_{ij} \delta_{kl} + 2E_s' \delta_{ij} \delta_{jl} \right] \times \alpha_{ij}(\mathbf{q}) \alpha_{kl}(-\mathbf{q}), \quad (2.14)$$

where  $\mathbf{q} = (q_1, q_2)$  is a three-dimensional wave vector. The kernel  $R_{ij,kl}(\mathbf{q})$  depends in a complicated way on the

elastic constants of the lattice. Its explicit expression is given in the Appendix with some details of the derivation. To evaluate  $F_D$  we have solved (2.6) with the condition that for a given configuration of dislocation lines the strain tensor  $w_{ik}(\mathbf{r})$  minimizes the free energy (2.12). We have also inserted in (2.14) terms containing the edge and screw dislocation core energies per unit length,  $E_e$ ,  $E_s$ , and  $E'_s$ . Although  $E'_s=0$  for a *single* dislocation line, we expect that a nonzero  $E'_s$  is required to describe short range interactions in the hydrodynamic limit. In making estimates we shall take  $E'_s \sim E_s$  for simplicity.

To study the properties of the flux-line lattice with dislocations we now need to calculate statistical-mechanical averages weighted with  $e^{-F_E/k_B T}$ . This involves integrating over the smoothly varying field  $\phi_{ij}(\mathbf{r})$  and summing over all distinct configurations of dislocation loops carrying allowed Burger's vectors. As discussed in Ref. 28, this second step is quite formidable if the discrete nature of the Burger's vectors is taken into account. On the other hand, in the long-wavelength limit we can disregard the discreteness of the Burger's vectors and treat  $\alpha_{ij}(\mathbf{r})$  as a continuous tensor field, subject only to the constraint (2.10). The presence of "unbound" dislocation loops of arbitrary size insures that  $\alpha_{ij}(\mathbf{q})$  can be regarded as a continuous tensor field in this hydrodynamic limit.<sup>28</sup> The statistical-mechanical averages can then be calculated by integrating over  $\alpha_{ij}(\mathbf{r})$ , with the constraint (2.10) that flux lines cannot start or stop inside the medium. In this sense dislocation lines are similar to magnetic field lines, which also are required to either close or terminate at the boundaries by the constraint of no magnetic monopoles.

### III. PROPERTIES OF THE HEXATIC LIQUID CRYSTAL PHASE

In this section we evaluate the renormalization of the elastic constants of the flux-line lattice due to dislocations and the correlations in the bond-angle field. We show that while dislocations drive the long-wavelength shear modulus to zero, i.e., melt the lattice, they do not destroy the long-range bond-orientational order of the crystal. A flux-line lattice with an equilibrium concentration of dislocation loops is therefore not a isotropic liquid, but a hexatic liquid crystal of lines in three dimension.

#### A. Renormalization of elastic constants

The renormalized Lamé coefficients are defined in terms of the components of the Fourier transform of the correlation function of the two-dimensional strain tensor,  $w_{ij}^{\perp}(\mathbf{r}) = \partial_i u_j$ , with  $i = x, y$  and  $j = x, y$ ,

$$G_{ij,kl}(q_{\perp}, q_z) = \langle w_{ij}^{\perp}(\mathbf{q}) w_{kl}^{\perp}(-\mathbf{q}) \rangle, \quad (3.1)$$

by

$$\frac{k_B T}{2\mu_R(q_{\perp}) + \lambda_R(q_{\perp})} = G_{ii,kk}(q_{\perp}, q_z = 0), \quad (3.2)$$

and

$$\frac{k_B T}{\mu_R(q_{\perp})} = G_{ik,ik}(q_{\perp}, q_z = 0) - G_{ii,kk}(q_{\perp}, q_z = 0), \quad (3.3)$$

where we shall ultimately be interested in the limit  $q_{\perp} \rightarrow 0$ . In the absence of dislocations the strain tensor correlation function is simply related to the correlation function of the smoothly varying part of the displacement field  $\phi(\mathbf{r})$ ,

$$G_{ij,kl}(q_{\perp}, q_z) = q_{\perp i} q_{\perp k} \langle \phi_j(\mathbf{q}) \phi_l(-\mathbf{q}) \rangle, \quad (3.4)$$

where

$$\langle \phi_i(\mathbf{q}) \phi_j(-\mathbf{q}) \rangle = k_B T \left[ \frac{Q_{ij}^{\perp}}{\mu q_{\perp}^2 + K q_z^2} + \frac{P_{ij}^{\perp}}{(2\mu + \lambda) q_{\perp}^2 + K q_z^2} \right]. \quad (3.5)$$

In Eq. (3.5) all indices run over the values  $x$  and  $y$ . The tensors  $Q_{ij}^{\perp}$  and  $P_{ij}^{\perp}$  are two-dimensional projection operators,

$$Q_{ij}^{\perp} = \delta_{ij} - \frac{q_{\perp i} q_{\perp j}}{q_{\perp}^2}, \quad (3.6)$$

$$P_{ij}^{\perp} = \frac{q_{\perp i} q_{\perp j}}{q_{\perp}^2}. \quad (3.7)$$

The Lamé coefficients defined in (3.2) and (3.3) are then independent of  $q_{\perp}$  and simply equal their bare values.

The renormalized tilt modulus is similarly related to the Fourier transform of the correlation function of the fluctuations in the tangent field,  $\mathbf{t}(\mathbf{r}) = \partial_z \mathbf{u}(\mathbf{r})$ , given by

$$T_{ij}(q_{\perp}, q_z) = \langle w_{zi}(\mathbf{q}) w_{zj}(-\mathbf{q}) \rangle. \quad (3.8)$$

The renormalized tilt modulus is then

$$\frac{k_B T}{2K_R(q_z)} = T_{ii}(q_{\perp} = 0, q_z), \quad (3.9)$$

where we are interested here in the limit  $q_z \rightarrow 0$ . The smoothly varying part of the tangent correlation function is simply,

$$T_{ij}(q_{\perp}, q_z) = q_z^2 \langle \phi_i(\mathbf{q}) \phi_j(-\mathbf{q}) \rangle, \quad (3.10)$$

and in the absence of dislocations  $K_R(q_z)$  as defined by (3.9) is independent of  $q_z$  and equals its bare value.

We now evaluate how the wave-vector-dependent elastic moduli defined by (3.2), (3.3), and (3.9) are renormalized by dislocations. The dislocation contribution to the correlation functions defined in (3.1) and (3.8) is determined by the singular part of the unsymmetrized strain tensor  $w_{ij}(\mathbf{r})$ , given in the Appendix in terms of the charge density tensor  $\alpha_{ij}(\mathbf{r})$ , Eq. (A9). The dislocation part of the strain and tangent correlation functions are then given in terms of the correlations of the charge-density tensor.

The calculation of the charge-density correlation functions is tedious, but straightforward. The constraint (2.10) is conveniently handled by adding a term

$$\frac{1}{2} M \int \frac{d\mathbf{q}}{(2\pi)^3} q_i \alpha_{ij}(\mathbf{q}) q_k \alpha_{kj}(-\mathbf{q}) \quad (3.11)$$

to the free energy (2.14) and taking the limit  $M \rightarrow \infty$  at the end of the calculation. The resulting correlation functions are given in the Appendix. After some algebra one finds that the renormalized bulk and shear moduli defined by (3.2) and (3.3) are given by

$$\frac{1}{2\mu_R(q_\perp) + \lambda_R(q_\perp)} = \frac{1}{2\mu + \lambda} \left[ 1 + \frac{2\mu^2}{2\mu(\mu + \lambda) + (2\mu + \lambda)E_e q_\perp^2} \right], \quad (3.12)$$

and

$$\frac{1}{\mu_R(q_\perp)} = \frac{1}{\mu} + \frac{1}{E_e q_\perp^2} + \frac{\lambda}{2\mu(\mu + \lambda) + (2\mu + \lambda)E_e q_\perp^2}. \quad (3.13)$$

While the renormalized bulk modulus is finite in the long wavelength limit, the renormalized shear modulus vanishes as  $q_\perp \rightarrow 0$ ,  $\lim_{q_\perp \rightarrow 0} \mu_R(q_\perp) = 0$ . In other words, dislocations destroy the long-range translational order in the  $xy$  plane and melt the lattice. It can be seen from Eq. (3.13) that edge dislocations are responsible for driving the shear modulus to zero as  $q_\perp \rightarrow 0$ . The screw dislocation energies appear when the relevant correlation functions are evaluated for  $q_z \neq 0$ . The compressional modulus (3.12) decreases to a finite value, as we would expect upon melting a solid.

The tangent correlation function splits into a longitudinal and a transverse part,

$$T_{ij}(q_\perp, q_z) = T_l(q_\perp, q_z)Q_{ij}^\perp + T_t(q_\perp, q_z)P_{ij}^\perp, \quad (3.14)$$

with

$$T_t(q_\perp, q_z) = \frac{k_B T}{K} \left[ 1 - \frac{2\mu q_\perp^2 E(\mathbf{q})}{K\mu[(4E_s + 2E_s')q_z^2 + E_e q_\perp^2] + 2E(\mathbf{q})D_1(\mathbf{q})} \right] \quad (3.15)$$

and

$$T_l(q_\perp, q_z) = \frac{k_B T}{K} \left[ 1 - \frac{2\mu(\mu + \lambda)q_\perp^2 + (2\mu + \lambda)q_\perp^2(E_e q_\perp^2 + 2E_s' q_z^2)}{2\mu(\mu + \lambda)q_\perp^2 + 2\mu K q_z^2 + (E_e q_\perp^2 + E_s' q_z^2)D_2(\mathbf{q})} \right], \quad (3.16)$$

where

$$D_1(\mathbf{q}) = Kq_z^2 + \mu q_\perp^2, \quad (3.17)$$

$$D_2(\mathbf{q}) = Kq_z^2 + (2\mu + \lambda)q_\perp^2, \quad (3.18)$$

and

$$E(\mathbf{q}) = E_e(E_s + E_s')q_\perp^2 + E_s'(2E_s + E_s')q_z^2. \quad (3.19)$$

One can see immediately from using (3.9) that the tilt modulus for  $q_\perp = 0$  is unchanged by dislocations, i.e.,

$$K_R(q_z) = K. \quad (3.20)$$

This is because dislocation loops of the kind considered here cannot relax a uniform tilt, as we show in the following.

The renormalization of the elastic constants by dislocations has its physical origin in the fact that dislocations can relax an applied stress by moving through the sample at the expense of plastic deformations of the crystal.<sup>30</sup> To gain some physical understanding of how dislocations change the elastic constants of the flux-line lattice it is useful to consider the force on a dislocation due to a uniform elastic stress matrix,  $\sigma_{ij}$ . This is the so-called Peach-Köhler force and can easily be evaluated. The only difference from standard treatments<sup>30</sup> is that the stress tensor of the flux-line lattice is not symmetric, as seen from Eqs. (A2) and (A3). The Peach-Köhler force is then found to be

$$f_i^\sigma(\mathbf{r}) = \sigma_{jk}(\mathbf{r})b_k \epsilon_{jil} \tau_l(\mathbf{r}). \quad (3.21)$$

Consider now a dislocation loop in the  $zx$  plane, i.e., with Burger's vector  $\mathbf{b} = b\hat{\mathbf{x}}$ . The force on the loop from a uniform external shear stress,  $\sigma_{jk} = \delta_{jy}\delta_{kx}\sigma_{yx}^0$ , is  $f_i^{\text{shear}} = \epsilon_{yil}\tau_l f_0^s$ , with  $f_0^s = \sigma_{yx}^0 b$ . For a circular loop this is a constant force directed radially outwards at each point on the loop. Its effect is to expand the dislocation loop out to the crystal boundaries. Dislocation loops are therefore very effective in relaxing shear and it is easy to understand how they can drive the shear modulus to zero.

We now consider the force on a loop with  $\mathbf{b} = b\hat{\mathbf{x}}$  resulting from applying a constant tilt to the lattice in the plane of the loop, i.e.,  $\sigma_{jk} = \delta_{jz}\delta_{kx}\sigma_{zx}^0$ . The resulting Peach-Köhler force is  $f_i^{\text{tilt}} = \epsilon_{zil}\tau_l f_0^t$ , with  $f_0^t = \sigma_{zx}^0 b$ . This force is always normal to the plane of the loop and there is no force on any segment of the loop that is parallel to the  $z$  axis. For a rectangular loop the force is nonzero only along the two segments parallel to the  $x$  axis. For  $\tau = \hat{\mathbf{x}}$ , we find  $f^{\text{tilt}} = -f_0^t \hat{\mathbf{y}}$  and for  $\tau = -\hat{\mathbf{x}}$ ,  $f^{\text{tilt}} = +f_0^t \hat{\mathbf{y}}$ . The Peach-Köhler force acts as a couple and tries to rotate the loop to bring it in the  $xy$  plane. Such a rotation is, however, not allowed by the geometrical restriction that dislocation loops must lie in the plane of  $\mathbf{b}$  and  $\mathbf{H}$ . Such motions are possible only if we allow flux-line cutting. As a consequence, dislocation loops cannot relax a tilt and the tilt modulus  $K$  is unchanged by dislocations.

As mentioned, we have neglected the nonlocality effects arising in the elastic properties of the flux line lattice from the long-range character of the interaction be-

tween flux lines. As discussed by Brandt,<sup>21</sup> this gives rise to a wave vector dependence of the elastic constants that is negligible only at wavelengths longer than the effective London penetration length,  $\lambda_L$ , which represents the range of the interaction and is usually much larger than the typical intervortex spacing  $d \sim n_0^{-1/2}$ . Here  $n_0 = B/\phi_0$  is the two-dimensional density of vortices, with  $\phi_0 = 2\pi\hbar c/2e$  the flux quantum. Within an isotropic approximation that neglects the angular dependence of the nonlocality (and neglecting as well the anisotropy of the critical masses in the high- $T_c$  superconductors), one finds<sup>21</sup> that the shear modulus  $\mu$  is independent of wave vector, while the compressional modulus  $2\mu + \lambda$  and the tilt modulus  $K$  are only functions of the magnitude  $q = |\mathbf{q}|$ . The compressional modulus exhibits a strong nonlocality and decreases considerably at large wave vectors. At  $q=0$ ,  $2\mu + \lambda \gg \mu$ , while for wavelengths of the order of the intervortex spacing  $d$ , one finds  $2\mu + \lambda \sim \mu$ . Nonlocality becomes important for  $q > \lambda_L^{-1} \ll d^{-1}$  and can be accounted for by replacing  $\mu$ ,  $\lambda$ , and  $K$  by their wave-vector-dependent counterparts.<sup>21</sup> Our main conclusion that dislocations melt the flux-line lattice by driving the long-wavelength shear modulus to zero will remain unchanged. The finding discussed in the follow-

ing that dislocations leave intact the long-range orientational order of the lattice will be unaffected by including nonlocality effects in the elasticity theory as well.

### B. Fluctuations in the bond-angle field

We are also interested in fluctuations in the bond-angle field,<sup>32</sup>

$$\theta(\mathbf{r}) = \frac{1}{2} \epsilon_{ij} w_{ij}^\perp(\mathbf{r}), \quad (3.22)$$

which gives the total twist in the material about the  $z$  axis. In the absence of dislocations the bond-angle field is slaved to the displacement field and equal to  $\frac{1}{2}(\partial_x u_y - \partial_y u_x)$ . Inserting (A9) into Eq. (3.22) we can express the bond-angle field more generally in terms of fluctuations in the smoothly varying part of the stress tensor and of the dislocation density tensor  $\alpha_{ij}(\mathbf{r})$ . We can then immediately evaluate the Fourier transform of the bond-angle correlation function,

$$\Theta(q_1, q_z) = \langle \theta(\mathbf{q}) \theta(-\mathbf{q}) \rangle, \quad (3.23)$$

with the result

$$\Theta(q_1, q_z) = \frac{k_B T}{4D_1(\mathbf{q})} \left[ q_1^2 + \frac{2K\mu D_1(\mathbf{q}) + E_e K^2 q_z^2 q_1^2 / 4 + 2(2E_s + E'_s) \mu^2 q_1^4}{K\mu[(4E_s + 2E'_s)q_z^2 + E_e q_1^2] + 2E(\mathbf{q})D_1(\mathbf{q})} \right], \quad (3.24)$$

where  $D_1(\mathbf{q})$  and  $E(\mathbf{q})$  are given in (3.17) and (3.19), respectively. The first term in large parentheses on the right-hand side of (3.24) is the contribution from the smoothly varying part of the displacement field, the second term is the contribution from dislocations. In order to display the limiting behavior of the bond-angle correlation function at long wavelength, it is instructive to rewrite (3.24) as

$$\Theta(q_1, q_z) = \frac{k_B T}{4(2E_s + E'_s)q_z^2 + 2E_e q_1^2} \frac{K\mu + \mu(2E_s + E'_s)q_1^2 + KE_e q_1^2 / 2 + E'_s D_1(\mathbf{q}) + E(\mathbf{q})q_1^2}{K\mu + 2D_1(\mathbf{q})E(\mathbf{q})q_1^2 / [2(2E_s + E'_s)q_z^2 + E_e q_1^2]}. \quad (3.25)$$

The bond-angle correlation function  $\Theta(q_1, q_z)$  is a singular function of  $\mathbf{q}$ . At small wave vectors it diverges as  $1/q^2$ , regardless of the direction along which the point  $\mathbf{q}=0$  is approached in the  $(q_1, q_z)$  plane. This signifies that the broken orientational symmetry of the crystal in the  $xy$  plane remains broken even in the presence of a finite density of unbound dislocation loops. The loops destroy the long-range translational order and drive the shear modulus to zero, but they leave the sixfold orientational symmetry of the triangular lattice in the  $xy$  plane intact. The flux-line lattice with an equilibrium concentration of dislocation loops is therefore not a isotropic liquid, but a hexatic liquid crystal of lines, with a solid-like resistance to torsion in the  $xy$  plane. It differs, however, from a two-dimensional hexatic in that the bond-orientational order is truly long ranged, as expected in three dimensions. This can be seen by considering the correlations of the bond-orientational order parameter,  $\psi_6(\mathbf{r}) = e^{6i\theta(\mathbf{r})}$ . The corresponding angular correlation function is

$$C_6(\mathbf{r}_1, z) = \langle e^{6i[\theta(\mathbf{r}) - \theta(0)]} \rangle = \exp\{-18\langle [\delta\theta(\mathbf{r})]^2 \rangle\}, \quad (3.26)$$

where  $\delta\theta(\mathbf{r}) = \theta(\mathbf{r}) - \theta(0)$  and  $\mathbf{r} = (\mathbf{r}_1, z)$ . The correlation function of the bond-angle field fluctuations in real space is

$$\langle [\delta\theta(\mathbf{r})]^2 \rangle = 2 \sum_{\mathbf{q}} [1 - \cos(\mathbf{q} \cdot \mathbf{r})] \Theta(q_1, q_z). \quad (3.27)$$

At large distances, i.e., as  $r_1 \rightarrow \infty$  and  $z \rightarrow \infty$ ,  $\langle [\delta\theta(\mathbf{r})]^2 \rangle$  goes to a cutoff-dependent constant,

$$\langle [\delta\theta(\mathbf{r})]^2 \rangle \rightarrow A \frac{k_B T \Lambda_1}{4\pi [2E_e(2E_s + E'_s)]^{1/2}}, \quad (3.28)$$

where  $\Lambda_1 = \sqrt{4\pi n_0}$  is a circular cutoff in the  $(q_x, q_y)$  plane and  $A$  is a constant of order unity. This is the signature of long-range order in the parameter  $\psi_6(\mathbf{r})$ . Long-range orientational order is plausible because the orientation of the triangles connecting nearest-neighbor

flux lines in Fig. 2 are essentially unaffected by the presence of the dislocation loop. The correlation function  $C_6(\mathbf{r}_1, z)$  decays algebraically to its asymptotic constant value. Evaluating the inverse Fourier transform on the right-hand side of (3.27) for large distances, one finds,

$$C_6(\mathbf{r}_1, z) \approx \exp \left[ -18A \frac{k_B T \Lambda_\perp}{4\pi [2E_e(2E_s + E'_s)]^{1/2}} \right] \times \left[ 1 + \frac{9k_B T}{2\pi \sqrt{E_e}} \frac{1}{\sqrt{(4E_s + 2E'_s)r_1^2 + E_e z^2}} \right]. \quad (3.29)$$

For points separated primarily along the  $z$  direction there is a  $1/z$  approach to the constant value,

$$C_6(\mathbf{r}_1, z) \underset{z \rightarrow \infty}{\approx} \exp \left[ -18A \frac{k_B T \Lambda_\perp}{4\pi [2E_e(2E_s + E'_s)]^{1/2}} \right] \times \left[ 1 + \frac{\xi_6^z}{z} \right], \quad (3.30)$$

where the orientational correlation length  $\xi_6^z$ ,

$$\xi_6^z = \frac{9k_B T}{2\pi E_e}, \quad (3.31)$$

is the scale over which the orientational order parameter of the flux lattice relaxes to its equilibrium value along the  $z$  direction. Similarly one finds a  $1/r_\perp$  algebraic decay for large separations in the  $xy$  plane,

$$C_6(\mathbf{r}_1, z) \underset{r_1 \rightarrow \infty}{\approx} \exp \left[ -18A \frac{k_B T \Lambda_\perp}{4\pi [2E_e(2E_s + E'_s)]^{1/2}} \right] \times \left[ 1 + \frac{\xi_6^\perp}{r_1} \right], \quad (3.32)$$

with a correlation length,

$$\xi_6^\perp = \frac{9k_B T}{2\pi \sqrt{2E_e(2E_s + E'_s)}}. \quad (3.33)$$

To evaluate the core energies per unit length that determine the correlation lengths  $\xi_6^z$  and  $\xi_6^\perp$  one needs a microscopic model of the dislocations. An upper bound for these energies can, however, be estimated by assuming that the strains in the dislocation core of cross section  $\sim b^2$  are of order unity.<sup>31</sup> One finds then  $E_e \sim \mu b^2$  and  $E_s \sim E'_s \sim \sqrt{K} \mu b^2$ , so that

$$\frac{\xi_6^z}{\xi_6^\perp} = \left[ \frac{2(2E_s + E'_s)}{E_e} \right]^{1/2} \approx \left[ \frac{K}{\mu} \right]^{1/4}. \quad (3.34)$$

It should be possible to see the hexatic phase by probing correlations between the flux lines by neutron scattering. In an isotropic flux liquid of rigid flux lines the scattering would give diffuse rings in the  $(q_x, q_y)$  plane, but would be sharp along  $q_z$ . In a disentangled hexatic phase of rigid lines, the diffuse rings in the  $(q_x, q_y)$  plane

will be modulated by the sixfold orientational order, but still be sharp in the  $q_z$  direction.<sup>33</sup> In the entangled state of both the liquid and the hexatic the rings will be diffuse along  $q_z$  because of the short-range correlations in the  $z$  direction induced by entanglement.<sup>1</sup> In the thermodynamic limit considered here the flux line hexatic is always entangled. In systems of a finite size in the  $z$  direction both an entangled and a disentangled hexatic regimes could exist. For fixed system size, the (possibly smooth) transition from disentangled to entangled state will take place as the density of flux lines is increased by increasing the external magnetic field.

In a phenomenological Landau-type description the long-range order in the bond-angle field can be incorporated by saying that there is an extra term in the long-wavelength free energy which resists deformations in  $\theta(\mathbf{r})$ , namely,

$$\delta F_H = \frac{1}{2} \int d\mathbf{r} [K_\perp |\nabla_\perp \theta|^2 + K_z (\partial_z \theta)^2]. \quad (3.35)$$

The stiffness parameters  $K_\perp$  and  $K_z$  are analogous to the Frank constants in a nematic liquid crystal. The free energy (3.35) is consistent with (2.14) at long wavelengths, provided

$$K_\perp = 2E_e, \quad K_z = 8E_s + 2E'_s. \quad (3.36)$$

The long-range orientational order will be destroyed at still higher temperatures by the proliferation of unbound disclinations. The flux-line lattice with an equilibrium concentration of both unbound dislocation loops and unbound disclinations will presumably be the entangled isotropic liquid of lines studied in Ref. 2.

In a perfect flux-line lattice without dislocations the deviation  $\delta n(\mathbf{r}) = n(\mathbf{r}) - n_0$  of the two-dimensional density of vortex lines,  $n(\mathbf{r})$ , from its equilibrium value,  $n_0$ , is related to the displacement  $\mathbf{u}(\mathbf{r})$  by  $\delta n(\mathbf{r}) = -n_0 \nabla_\perp \cdot \mathbf{u}(\mathbf{r})$ . When there are no dislocations in the lattice and  $\mathbf{u}(\mathbf{r})$  is smoothly varying the tangent fluctuations  $\mathbf{t}(\mathbf{r})$  satisfy a sort of continuity equation in the timelike variable  $z$ ,

$$\partial_z \delta n(\mathbf{r}) = -n_0 \nabla_\perp \cdot \mathbf{t}(\mathbf{r}), \quad (3.37)$$

since

$$\partial_z [\nabla_\perp \cdot \mathbf{u}(\mathbf{r})] = \nabla_\perp \cdot \mathbf{t}(\mathbf{r}).$$

Equation (3.37) still applies in the presence of dislocations as long as the constraint (2.8) holds, i.e., provided there are no half lines or "vacancies" in the lattice. The *longitudinal* part of the correlation function of tangent fluctuations (3.16) is therefore directly related to the correlation function of fluctuations in the flux-line density.

When screw dislocations are present, the *transverse* part of  $\mathbf{t}(\mathbf{r})$  is an independent physical variable that characterizes entanglement. It is useful to introduce a "vorticity" field  $\mathbf{m}(\mathbf{r})$  which describes the braiding of the flux lines along the  $z$  axis, namely,

$$\mathbf{m}(\mathbf{r}) = \frac{1}{2} \hat{\mathbf{z}} \cdot [\nabla_\perp \times \mathbf{t}(\mathbf{r})]. \quad (3.38)$$



In the absence of dislocations we have simply,

$$m(\mathbf{r}) = \partial_z \theta(\mathbf{r}). \quad (3.39)$$

When screw dislocations are present (3.39) is, however, replaced by

$$m(\mathbf{r}) = \partial_z \theta(\mathbf{r}) + \frac{1}{2} \alpha_{ii}^{\perp}(\mathbf{r}). \quad (3.40)$$

Equation (3.40) arises because both screw dislocations and explicit twisting of the bond-angle field contribute to the ‘‘vorticity.’’ The physics contained in (3.37) and (3.40) is important for constructing a theory of the dynamics of the entangled hexatic of flux lines.<sup>34</sup>

*Note added in proof.* After this paper was accepted for publication, we received a report preprint from T. K. Worthington, F. H. Holtzberg, and C. A. Field (IBM report, that presents evidence from resistivity data for two liquid regimes above the melting line in Y-Ba-Cu-O, one of which is identified with the entangled hexatic line liquid discussed here.

#### ACKNOWLEDGMENTS

We have benefitted from conversations with J. Socolar and P. Ginsparg. This work was supported by the National Science Foundation at Syracuse University through Grant No. DMR87-17337 and at Harvard University through the Material Research Laboratory and through Grant No. DMR88-17291.

#### APPENDIX: THE FREE ENERGY OF DISLOCATIONS

In this appendix we obtain the dislocation free energy (2.14). For clarity in this section we will use roman letters  $i, j, k, \dots$  to denote indices that only run over the values  $x$  and  $y$  and greek letters,  $\alpha, \beta, \gamma, \dots$  to denote indices that run over  $x, y, z$ . We need to find the singular part of the strain tensor,  $w_{\beta i}(\mathbf{r})$ , due to an equilibrium distribution of dislocation loops characterized by the density tensor  $\alpha_{\beta i}(\mathbf{r})$ . This is given by the solution of (2.6) which also minimizes the elastic free energy, i.e., satisfies the condition

$$\partial_\alpha \sigma_{\alpha i}(\mathbf{r}) = 0, \quad (A1)$$

$$F_D = \frac{1}{2} \int \frac{d\mathbf{q}}{(2\pi)^3} \left[ \frac{1}{q^2} R_{\beta i, \gamma j}(\mathbf{q}) + 2E_e \delta_{ij} \delta_{\beta z} \delta_{\gamma z} + 2E_s \delta_{\beta i} \delta_{\gamma j} + 2E'_s (\delta_{\beta \gamma} - \delta_{\beta z} \delta_{\gamma z}) \delta_{ij} \right] \alpha_{\beta i}(\mathbf{q}) \alpha_{\gamma j}(-\mathbf{q}), \quad (A10)$$

with

$$R_{\beta i, \gamma j}(\mathbf{q}) = C_{\beta \alpha} [-C_{\alpha i \mu j} + C_{\alpha i \eta k q \eta} (A^{-1})_{kl} q_\nu C_{\nu l \mu j}] C_{\mu \gamma}, \quad (A11)$$

and  $C_{\alpha \beta} = \epsilon_{\alpha \beta \gamma} q_\gamma / q$ . The explicit expression of the dislocation free energy (A10) is

$$F_D = \frac{1}{2} \int \frac{d\mathbf{q}}{(2\pi)^3} \left[ \frac{1}{q^2} \{ G_{i,j}^{zz}(\mathbf{q}) \alpha_{zi}(\mathbf{q}) \alpha_{zj}(-\mathbf{q}) + G_{i,jk}^{z\perp}(\mathbf{q}) [\alpha_{zi}(\mathbf{q}) \alpha_{kj}^{\perp}(-\mathbf{q}) + \alpha_{zi}(-\mathbf{q}) \alpha_{kj}^{\perp}(\mathbf{q})] + G_{ki,lj}^{\perp\perp}(\mathbf{q}) \alpha_{ki}^{\perp}(\mathbf{q}) \alpha_{lj}^{\perp}(-\mathbf{q}) \} \right. \\ \left. + 2E_e \delta_{ij} \alpha_{zi}(\mathbf{q}) \alpha_{zj}(-\mathbf{q}) + (2E_s \delta_{ik} \delta_{jl} + 2E'_s \delta_{ij} \delta_{kl}) \alpha_{ki}^{\perp}(\mathbf{q}) \alpha_{lj}^{\perp}(-\mathbf{q}) \right], \quad (A12)$$

where

$$G_{i,j}^{zz}(\mathbf{q}) = \frac{q^2}{q^2} \left[ \left( 2\mu + \lambda \frac{2\mu q_1^2 + K q_z^2}{D_2(\mathbf{q})} \right) Q_{ij}^{\perp} + \frac{\mu K q_z^2}{D_1(\mathbf{q})} P_{ij}^{\perp} \right], \quad (A13)$$

where  $\sigma_{\alpha i}(\mathbf{r})$  is the stress tensor,

$$\sigma_{\alpha i}(\mathbf{r}) = C_{\alpha i \beta j} w_{\beta j}(\mathbf{r}), \quad (A2)$$

with  $C_{\alpha i \beta j}$  the elastic tensor

$$C_{\alpha i \beta j} = \mu [(\delta_{\alpha \beta} - \delta_{\alpha z} \delta_{\beta z}) \delta_{ij} + \delta_{\alpha j} \delta_{\beta i}] \\ + \lambda \delta_{\alpha i} \delta_{\beta j} + K \delta_{\alpha z} \delta_{\beta z} \delta_{ij}. \quad (A3)$$

It is convenient to work in Fourier space. Equation (2.6) becomes then

$$\epsilon_{\beta \gamma \eta} i q_\gamma w_{\eta i}(\mathbf{q}) = \alpha_{\beta i}(\mathbf{q}), \quad (A4)$$

which has solution,

$$w_{\alpha i}(\mathbf{q}) = -\frac{i}{q^2} \epsilon_{\alpha \beta \gamma} q_\beta \alpha_{\gamma i}(\mathbf{q}) + i q_\alpha \psi_i(\mathbf{q}). \quad (A5)$$

The two unknown functions  $\psi_i(\mathbf{q})$ , for  $i=x, y$  are determined by requiring that (A5) satisfies (A1), i.e., the distribution of dislocations is an equilibrium one. One finds

$$\psi_i(\mathbf{q}) = \frac{1}{q^2} (A^{-1})_{ij} q_\alpha C_{\alpha j \beta k} \epsilon_{\beta \gamma \eta} q_\gamma \alpha_{\eta k}(\mathbf{q}), \quad (A6)$$

where  $A$  is a  $2 \times 2$  matrix defined by

$$A_{ij} = q_\alpha q_\beta C_{\alpha i \beta j} \\ = D_1(\mathbf{q}) \delta_{ij} + (\mu + \lambda) q_{\perp i} q_{\perp j}. \quad (A7)$$

The inverse matrix is given by

$$(A^{-1})_{ij} = \frac{1}{D_1(\mathbf{q})} \left[ \delta_{ij} - \frac{\mu + \lambda}{D_2(\mathbf{q})} q_{\perp i} q_{\perp j} \right]. \quad (A8)$$

The functions  $D_1(\mathbf{q})$  and  $D_2(\mathbf{q})$  have been defined in (3.17) and (3.18). Substituting (A6) in (A5), the desired solution is

$$w_{\alpha i}(\mathbf{q}) = -\frac{i}{q^2} [\epsilon_{\alpha \beta \gamma} q_\beta \delta_{ij} \\ - q_\alpha (A^{-1})_{ik} q_\beta C_{\beta k \rho j} \epsilon_{\rho \eta \gamma} q_\eta \alpha_{\gamma j}(\mathbf{q})]. \quad (A9)$$

Finally, substituting (A9) in the elastic free energy we obtain,

and

$$G_{i,kj}^{z\perp}(\mathbf{q}) = \frac{q_z q_\perp}{q^2} \left[ -\mu Q_{ij}^\perp \hat{q}_\perp k - \mu C_k^\perp \epsilon_{ij} - \frac{\mu K q_z^2}{D_1(\mathbf{q})} P_{ij}^\perp \hat{q}_{\perp k} + \frac{\lambda(K-2\mu)q_\perp^2}{D_2(\mathbf{q})} Q_{ik}^\perp \hat{q}_{\perp j} + \frac{\mu(K-\mu)q_\perp^2}{D_1(\mathbf{q})} Q_{jk}^\perp \hat{q}_{\perp i} \right], \quad (\text{A14})$$

and

$$G_{ki,lj}^{\perp\perp}(\mathbf{q}) = \frac{q_z^2}{q^2} \left[ \left[ \mu + K \frac{q_\perp^2}{q_z^2} - \frac{(K-\mu)^2 q_\perp^2}{D_1(\mathbf{q})} \right] Q_{ij}^\perp Q_{kl}^\perp + \mu Q_{ij}^\perp P_{kl}^\perp + \mu \epsilon_{jk} \epsilon_{il} \right. \\ \left. + \left[ \mu + K \frac{q_\perp^2}{q_z^2} - 2\mu \frac{(K-\mu)q_\perp^2}{D_1(\mathbf{q})} - \frac{(K-2\mu)^2 q_\perp^2}{D_2(\mathbf{q})} \right] P_{ij}^\perp Q_{kl}^\perp \right. \\ \left. + \frac{\mu K q_z^2}{D_1(\mathbf{q})} P_{ij}^\perp P_{kl}^\perp - \frac{\mu(K-\mu)q_\perp^2}{D_1(\mathbf{q})} (\hat{q}_\perp i C_j^\perp \epsilon_{jk} + \hat{q}_\perp j C_k^\perp \epsilon_{il}) \right]. \quad (\text{A15})$$

Here we have defined a unit vector of components  $\hat{q}_{\perp i} = q_{\perp i} / q_\perp$ , for  $i = x, y$ , and  $C_i^\perp = \epsilon_{ij} q_{\perp j} / q_\perp$ .

All physical quantities of interest here can be expressed in terms of the smoothly varying part of the displacement field  $\phi(\mathbf{r})$  and the dislocation density tensor  $\alpha_{\beta i}(\mathbf{r})$ . The correlation function of the strain tensor can therefore be written as a ‘‘regular’’ part, given in (3.4) and a part due to dislocations which is expressed in terms of the correlation function of the dislocation density tensor. The latter is easily evaluated within the continuum approximation described in Sec. II where the statistical average over the dislocation density is performed by regarding  $\alpha_{\beta i}(\mathbf{r})$  as a continuum tensor field. The calculation is lengthy, but straightforward. To perform the integrations over the three independent components of the tensor  $\alpha_{ij}^\perp(\mathbf{q})$ , we decompose this symmetric  $2 \times 2$  tensor as

$$\alpha_{ij}^\perp(\mathbf{q}) = Q_{ij}^\perp \alpha_1(q_\perp, q_z) + \hat{q}_{\perp i} h_j(\mathbf{q}) + \hat{q}_{\perp j} h_i(\mathbf{q}), \quad (\text{A16})$$

where  $\mathbf{h}(\mathbf{q})$  is an arbitrary two-component vector, i.e.,

$$h_i(\mathbf{q}) = \hat{q}_{\perp i} \alpha_2(q_\perp, q_z) + C_i^\perp \alpha_3(q_\perp, q_z), \quad (\text{A17})$$

with  $\alpha_n(q_\perp, q_z)$ , for  $n = 1, 2, 3$ , arbitrary scalar functions of  $q_\perp$  and  $q_z$ . The constraint (2.8) is then automatically incorporated in the calculation. The components of the correlation function of the dislocation density tensor are given by,

$$\langle \alpha_{zi}(\mathbf{q}) \alpha_{zj}(-\mathbf{q}) \rangle = k_B T \left[ Q_{ij}^\perp \frac{q_\perp^2}{R_2(\mathbf{q})} + P_{ij}^\perp \frac{[K\mu + 2(E_s + E'_s)D_1]q_\perp^2}{R_1(\mathbf{q})} \right], \quad (\text{A18})$$

and

$$\langle \alpha_{zi}(\mathbf{q}) \alpha_{kl}^\perp(-\mathbf{q}) \rangle = -k_B T \left[ Q_{kl}^\perp \hat{q}_{\perp i} \frac{(K\mu - 2E_s D_1)q_\perp q_z}{R_1(\mathbf{q})} + P_{kl}^\perp \hat{q}_{\perp i} \frac{[K\mu + 2(E_s + E'_s)D_1]q_\perp q_z}{R_1(\mathbf{q})} + (Q_{il}^\perp \hat{q}_{\perp k} + Q_{ik}^\perp \hat{q}_{\perp l}) \frac{p_\perp q_z}{R_2(\mathbf{q})} \right], \quad (\text{A19})$$

and

$$\langle \alpha_{ij}^\perp(\mathbf{q}) \alpha_{kl}^\perp(-\mathbf{q}) \rangle = k_B T \left[ (Q_{ij}^\perp Q_{kl}^\perp + P_{ij}^\perp P_{kl}^\perp) \frac{[K\mu + 2(E_s + E'_s)D_1]q_z^2}{R_1(\mathbf{q})} \right. \\ \left. + Q_{ij}^\perp Q_{kl}^\perp \frac{2E_s q_\perp^2 D_1}{R_1(\mathbf{q})} + (Q_{ij}^\perp P_{kl}^\perp + P_{ij}^\perp Q_{kl}^\perp) \frac{(K\mu - 2E_s D_1)q_z^2}{R_1(\mathbf{q})} \right. \\ \left. + (Q_{jl}^\perp P_{ik}^\perp + Q_{il}^\perp P_{jk}^\perp + Q_{jk}^\perp P_{il}^\perp + Q_{ik}^\perp P_{jl}^\perp) \frac{q_z^2}{R_2(\mathbf{q})} \right], \quad (\text{A20})$$

where

$$R_1(\mathbf{q}) = K\mu[4(2E_s + E'_s)q_z^2 + 2E_e q_\perp^2] + 4E(\mathbf{q})D_1(\mathbf{q}), \quad (\text{A21})$$

$$R_2(\mathbf{q}) = 2\mu \left[ 1 + \frac{\lambda q_\perp^2 + K q_z^2}{D_2(\mathbf{q})} \right] + 2E_e q_\perp^2 + 4E'_s q_z^2, \quad (\text{A22})$$

and  $E(\mathbf{q})$  has been defined in (3.19).

- \*On leave from Physics Department, Syracuse University, Syracuse, NY 13244.
- <sup>1</sup>D. R. Nelson, Phys. Rev. Lett. **60**, 1973 (1988).
- <sup>2</sup>D. R. Nelson and S. Seung, Phys. Rev. B **39**, 9153 (1989).
- <sup>3</sup>M. P. A. Fisher and D. H. Lee, Phys. Rev. B **39**, 2756 (1989).
- <sup>4</sup>M. P. A. Fisher, Phys. Rev. Lett. **62**, 1415 (1989).
- <sup>5</sup>A. Houghton, R. A. Pelcovits, and A. Sudbo, Phys. Rev. B **40**, 6763 (1989).
- <sup>6</sup>P. L. Gammel, D. J. Bishop, G. J. Dolan, J. R. Kwo, C. A. Murray, L. F. Schneemeyer, and J. V. Waszczak, Phys. Rev. Lett. **59**, 2592 (1987).
- <sup>7</sup>P. L. Gammel, L. F. Schneemeyer, J. V. Waszczak, and D. J. Bishop, Phys. Rev. Lett. **61**, 1666 (1988).
- <sup>8</sup>D. R. Nelson, J. Stat. Phys. (to be published).
- <sup>9</sup>See also, D. Huse, M. P. A. Fisher, and D. S. Fisher (unpublished).
- <sup>10</sup>M. Tinkham, Helv. Phys. Acta **61**, 443 (1988); Phys. Rev. Lett. **61**, 1658 (1988).
- <sup>11</sup>A. I. Larkin, Zh. Eksp. Teor. Fiz. **58**, 1466 (1970) [Sov. Phys.-JETP **31**, 784 (1970)]; A. I. Larkin and Y. N. Ovchinnikov, J. Low Temp. Phys. **34**, 409 (1979).
- <sup>12</sup>G. J. Dolan, G. V. Chandrasekar, T. R. Dinger, C. Field, and F. Holtzberg, Phys. Rev. Lett. **62**, 827 (1989).
- <sup>13</sup>Such a scenario is suggested by the striking low-field photographs that recently appeared in R. N. Kleiman, P. L. Gammel, L. F. Schneemeyer, J. V. Waszczak, and D. J. Bishop, Phys. Rev. Lett. **62**, 2331 (1989).
- <sup>14</sup>E. H. Brandt, P. Esquinazi, and G. Weiss, Phys. Rev. Lett. **62**, 2330 (1989).
- <sup>15</sup>D. S. Fisher, Phys. Rev. B **22**, 1190 (1980).
- <sup>16</sup>See, for instance, A. L. Fetter and P. C. Hohenberg, in *Superconductivity*, edited by R. D. Parks (Dekker, New York, 1969), Vol. 2.
- <sup>17</sup>A similar picture has been proposed for defect lines in metallic glasses: See D. R. Nelson and F. Spaepen, Solid State Phys. **42**, 1 (1989).
- <sup>18</sup>A. P. Malozemoff, T. K. Worthington, Y. Yeshurun, and F. Holtzberg, Phys. Rev. B **38**, 7203 (1988), and references therein.
- <sup>19</sup>R. Wördenweber and P. H. Kes, Phys. Rev. B **34**, 494 (1986).
- <sup>20</sup>E. H. Brandt, Phys. Rev. B **34**, 6514 (1986); Jpn. J. Appl. Phys. **26**, 1515 (1987).
- <sup>21</sup>E. H. Brandt and U. Essman, Phys. Status Solidi B **144**, 13 (1987).
- <sup>22</sup>For a review of these ideas and an interesting attempt to justify Eq. (1.1), see T. Yamamoto and T. Izuyama, J. Phys. Soc. Jpn. **57**, 3742 (1988).
- <sup>23</sup>E. Brézin, D. R. Nelson, and A. Thiaville, Phys. Rev. B **31**, 7124 (1985).
- <sup>24</sup>Strictly speaking, these dislocations are not quite the same as those discussed in Refs. 20 and 21. In Brandt's picture, screw dislocations will enter a sample whose crystalline order in any  $xy$  plane has already been disrupted by the quenched random impurity potential: any constant- $z$  cross section initially have a finite concentration of edge dislocations and disclinations. The dislocation loops we consider have a mixed edge and screw character, and disrupt a lattice which is initially crystalline in any constant- $z$  cross section. This insures that the Burger's vectors have a well-defined magnitude and direction.
- <sup>25</sup>F. R. N. Nabarro and A. T. Quintanilha, in *Dislocations in Solids*, edited by F. R. N. Nabarro (North-Holland, Amsterdam, 1980), Vol. 5. For important early work on this subject, see, e.g., R. Labusch, Phys. Lett. **22**, 9 (1966).
- <sup>26</sup>D. R. Nelson and B. I. Halperin, Phys. Rev. B **19**, 2457 (1979).
- <sup>27</sup>While this manuscript was in preparation, we received an interesting paper by Chudnovsky (unpublished), who proposes a hexatic *glass* phase at low temperatures. Chudnovsky observed that the random impurity disorder studied by Larkin and Ovchinnikov (Ref. 11) is insufficient to destroy long-range bond-orientational order, although it does disrupt translational correlations. Chudnovsky's model does not, however, allow for a random field which acts directly on the bond-angle field. Such a random field will be generated in realistic samples whenever two impurities in close proximity single out a preferred set of local crystallographic axes. Although this field will destroy long-range orientational order, the orientational correlation length could greatly exceed the translational correlation length in some samples, in qualitative agreement with Chudnovsky's ideas.
- <sup>28</sup>D. R. Nelson and J. Toner, Phys. Rev. B **24**, 363 (1981).
- <sup>29</sup>In the notation of Ref. 21, we have  $c_{44}=K$ ,  $c_{66}=\mu$ , and  $c_{11}=2\mu+\lambda$ .
- <sup>30</sup>L. D. Landau and E. M. Lifschitz, *Theory of Elasticity* (Pergamon, New York, 1970).
- <sup>31</sup>A. M. Kosevich, in *Dislocations in Solids*, edited by F. R. N. Nabarro (North-Holland, New York, 1979), Vol. 1.
- <sup>32</sup>For a review see D. R. Nelson, in *Phase Transitions and Critical Phenomena*, edited by C. Domb and J. L. Lebowitz (Academic, New York, 1983), Vol. 7.
- <sup>33</sup>R. Bruinsma and D. R. Nelson, Phys. Rev. B **23**, 402 (1981).
- <sup>34</sup>M. C. Marchetti and D. R. Nelson (unpublished).